

Supporting information to

Engineering the Interface in Mechanically Responsive

Graphene-Based Films

Yaqing Chen^{1,2}, Zhaohe Dai¹, Chuanxin Weng^{1,2}, Guorui Wang¹, Xuelu Liu³, Xin
Cong³, Pingheng Tan³, Luqi Liu^{*,1} and Zhong Zhang^{*,1}

¹ CAS Key Laboratory of Nanosystem and Hierarchical Fabrication, CAS Center for
Excellence in Nanoscience, National Center for Nanoscience and Technology,
Beijing, 100190, People's Republic of China

²University of Chinese Academy of Science, Beijing 100049, People's Republic of
China

³State Key Laboratory of Superlattices and Microstructures, Chinese Academy of
Sciences, Beijing 100083, People's Republic of China

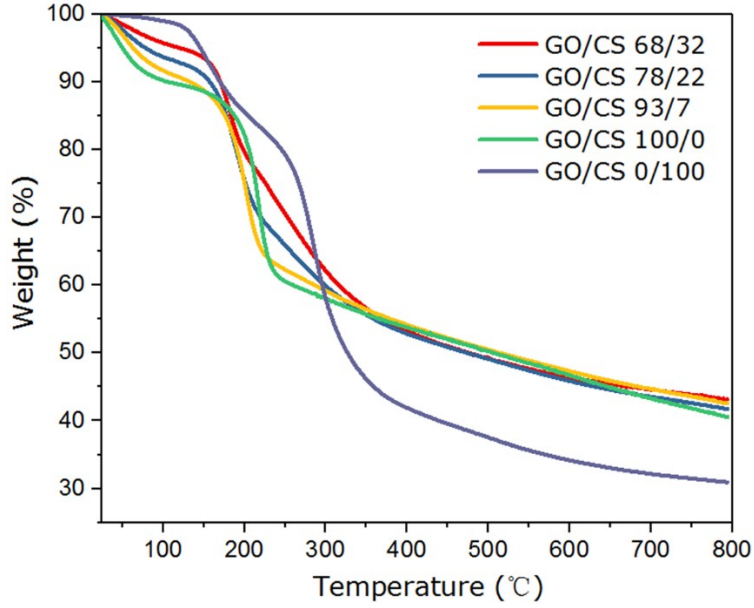


Fig. S1 TGA curves of GO/CS nanocomposite films with a heating rate of 10 °C/min under nitrogen atmosphere. Considering the weight loss before 105 °C is mainly due to water evaporating and both GO and CS have all degradation peaks before 500 °C, temperature ranging from 105 °C to 500 °C is chosen to calculate the GO weight fraction of GO/CS nanocomposites.

The calculation of GO weight percent (w) in GO/CS nanocomposites is decided by equation¹ S1:

$$w = \frac{M - M_{CS}}{M_{GO} - M_{CS}} \times 100\% \quad (S1)$$

w represents the GO weight percent; M , M_{GO} and M_{CS} are weight losses of GO/CS composites between 105 °C to 500 °C, respectively.

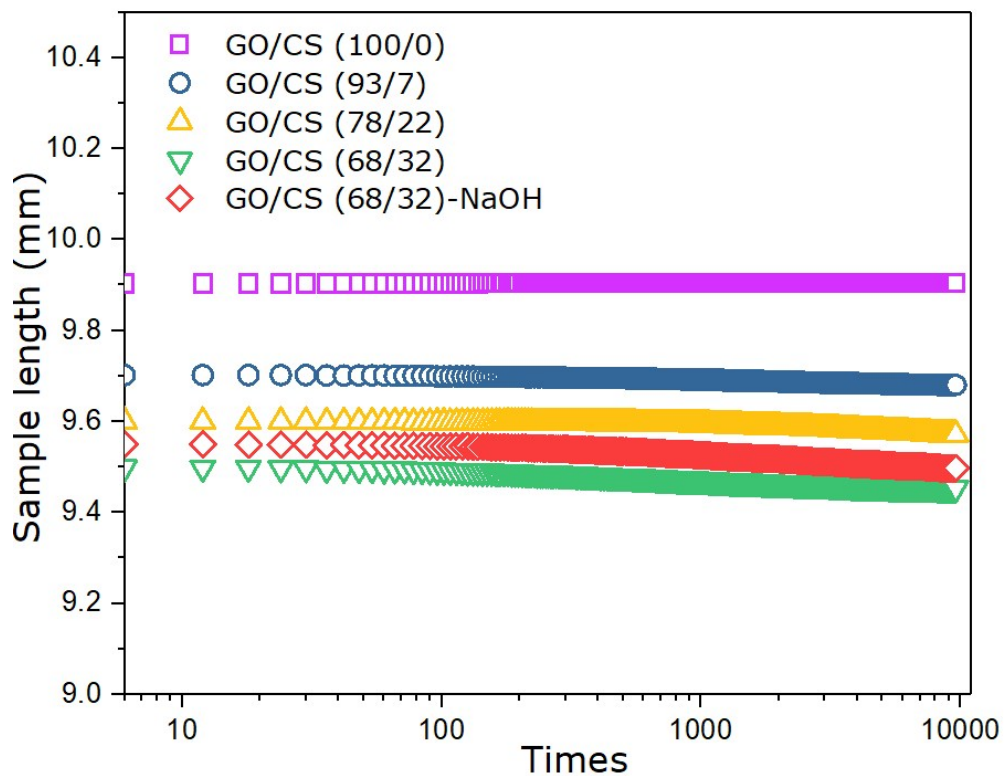


Fig. S2 Length changes of a series of GO/CS nanocomposite films with different weight ratios (100/0, 93/7, 78/22, 68/32) and alkali treated GO/CS (68/32) films during dynamic tension.

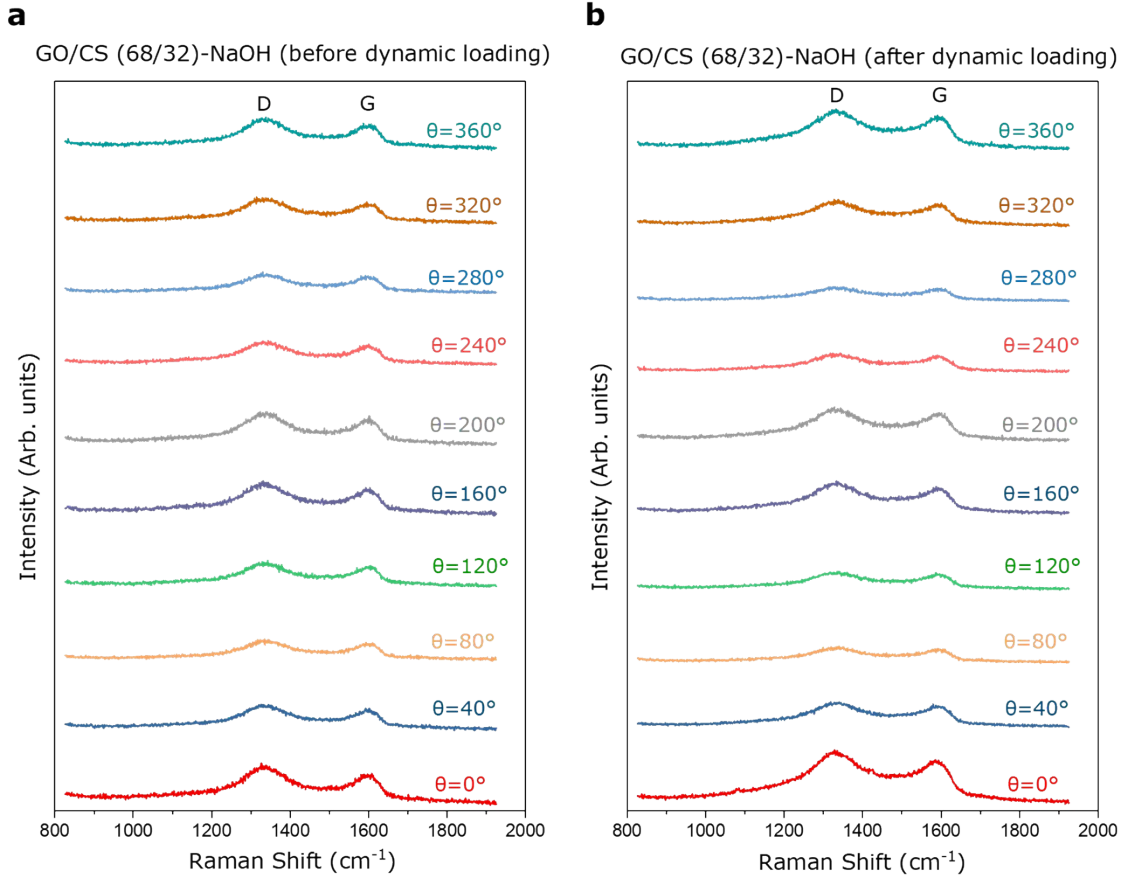


Fig. S3 Raman spectra of alkali treated GO/CS (68/32) films with varying polarization angles (θ) of incident laser for samples (a) before dynamic loading and (b) after dynamic loading. It is acknowledged that¹³

$$I_G(\alpha) = \frac{1}{2} c^2 \cos^2 \alpha \left\{ 2 + \cos [2(\alpha - \theta)] + \cos [2(\alpha + \theta)] \right\} \quad (S2)$$

I_G reaches a maximum value $I_G(\parallel)$ when the electric field vector is parallel to the base plane of the GO/CS (68/32)-NaOH film ($\theta=0^\circ$ and 180°), while arrives at a minimum value $I_G(\perp)$ when perpendicular to the base plane ($\theta=90^\circ$ and 270°). $I_G(\parallel)/I_G(\perp)$ is equal to $\cot^2\alpha$, indicating a decreasing α with an increasing ration of $I_G(\parallel)/I_G(\perp)$.

Table S1. The detailed peak information from XPS spectra of untreated and alkali treated GO and GO/CS films.

Functional groups	C1s					N1s		
	C in graphite (eV)	C-N (eV)	C-O (eV)	C=O (eV)	C(O)O (eV)	NH ₂ (eV)	O=C-N (eV)	NH ₃ ⁺ (eV)
GO	284.7 (52.7%)	---	286.8 (25.5%)	287.3 (10.6%)	288.6 (11.2%)	---	---	---
GO-NaOH	284.7 (72.6%)	---	286.4 (17.2%)	288.2 (10.2%)	---	---	---	---
GO/CS (68/32)	284.8 (39.6%)	286.2 (18.1%)	286.8 (20.4)	287.8 (15.3%)	288.3 (6.6%)	399.3 (53.6%)	399.9 (30.6%)	401.7 (15.8%)
GO/CS (68/32)-NaOH	284.7 (52.0%)	285.8 (14.6%)	286.4 (27.1%)	288.2 (6.3%)	---	399.7 (92.1%)	400.1 (7.9%)	---

Table S2. The mechanical properties of alkali treated GO-based films in our work and other GO-based nanocomposites reported in literatures.¹⁻¹²

Materials	Modulus (GPa)	Stress (MPa)	Toughness (MJ/m ³)	Reference
rGO-CS	6.5	526.7	17.7	1
GO-GA	30.0	101.0	0.3	2
GO-Ca ²⁺	28.1	125.8	0.3	3
GO-Mg ²⁺	27.9	80.6	0.2	3
GO-Al ³⁺	26.2	100.5	0.2	4
GO-PMMA	7.5	148.3	2.4	5
GO-PVA	10.4	188.9	2.5	5
rGO-PAPB	7.17	382.0	7.5	7
rGO-MoS ₂ -TPU	10.0	235.0	6.9	8
rGO-SL	26.0	300.0	0.8	9
rGO-MMT-PVA	2.5.0	356.0	7.4	10
GO-MMT-PVA	16.0	263.0	7.5	10
rGO-DWNTs-PVA	6.0	375.8	11.3	11
rGO-PCDO-NFC	2.5	314.6	9.8	12
GO	9.4±0.8	67.0±9.8	0.3±0.1	This work
GO/CS	12.7±1.3	170.7±15.2	2.8±0.3	This work
GO/CS-NaOH	20.9±3.5	316.0±31.7	6.0±0.9	This work
GO/CS-NaOH stressed	35.1±4.2	614.0±36.6	9.3±1.7	This work

References

- (1) Wan, S.; Peng, J.; Li, Y.; Hu, H.; Jiang, L.; Cheng, Q. Use of Synergistic Interactions to Fabricate Strong, Tough, and Conductive Artificial Nacre Based on Graphene Oxide and Chitosan. *ACS Nano* **2015**, *9* (10), 9830-9836.
- (2) Gao, Y.; Liu, L.-Q.; Zu, S.-Z.; Peng, K.; Zhou, D.; Han, B.-H.; Zhang, Z. The Effect of Interlayer Adhesion on the Mechanical Behaviors of Macroscopic Graphene Oxide Papers. *ACS Nano* **2011**, *5* (3), 2134-2141.
- (3) Park, S.; Lee, K.-S.; Bozoklu, G.; Cai, W.; Nguyen, S. T.; Ruoff, R. S. Graphene Oxide papers Modified by Divalent Ions-Enhancing Mechanical Properties via Chemical Cross-Linking. *ACS Nano* **2008**, *2* (3), 572-578.
- (4) Yeh, C. N.; Raidongia, K.; Shao, J.; Yang, Q. H.; Huang, J. On the Origin of the Stability of Graphene Oxide Membranes in Water. *Nat. Chem.* **2014**, *7* (2), 166-170.
- (5) Putz, K. W.; Compton, O. C.; Palmeri, M. J.; Nguyen, S. T.; Brinson, L. C. High-Nanofiller-Content Graphene Oxide Polymer Nanocomposites via Vacuum-Assisted Self-Assembly. *Adv. Funct. Mater.* **2010**, *20* (19), 3322-3329.
- (6) Li, Y. Q.; Yu, T.; Yang, T. Y.; Zheng, L. X.; Liao, K. Bio-Inspired Nacre-like Composite Films Based on Graphene with Superior Mechanical, Electrical, and Biocompatible Properties. *Adv. Mater.* **2012**, *24* (25), 3426-3431.
- (7) Tian, Y.; Cao, Y.; Wang, Y.; Yang, W.; Feng, J. Realizing Ultrahigh Modulus and High Strength of Macroscopic Graphene Oxide Papers through Crosslinking of Mussel-Inspired Polymers. *Adv. Mater.* **2013**, *25* (21), 2980-2983.
- (8) Wan, S.; Li, Y.; Peng, J.; Hu, H.; Cheng, Q.; Jiang, L. Synergistic Toughening of Graphene Oxide–Molybdenum Disulfide–Thermoplastic Polyurethane Ternary Artificial Nacre. *ACS Nano* **2015**, *9* (1), 708-714.
- (9) Hu, K.; Tolentino, L. S.; Kulkarni, D. D.; Ye, C.; Kumar, S.; Tsukruk, V. V. Written-in Conductive Patterns on Robust Graphene Oxide Biopaper by Electrochemical Microstamping. *Angew. Chem. Int. Ed.* **2013**, *52* (51), 13784-13788.
- (10) Ming, P.; Song, Z.; Gong, S.; Zhang, Y.; Duan, J.; Zhang, Q.; Jiang, L.; Cheng, Q. Nacre-Inspired Integrated Nanocomposites with Fire Retardant Properties by Graphene Oxide and Montmorillonite. *J. Mater. Chem. A* **2015**, *3* (42), 21194-21200.
- (11) Gong, S.; Cui, W.; Zhang, Q.; Cao, A.; Jiang, L.; Cheng, Q. Integrated Ternary Bioinspired Nanocomposites via Synergistic Toughening of Reduced Graphene Oxide and Double-Walled Carbon Nanotubes. *ACS Nano* **2015**, *9* (12), 11568-11573.

(12) Duan, J.; Gong, S.; Gao, Y.; Xie, X.; Jiang, L.; Cheng, Q. Bioinspired Ternary Artificial Nacre Nanocomposites Based on Reduced Graphene Oxide and Nanofibrillar Cellulose. *ACS Appl. Mater. Interfaces* **2016**, *8* (16), 10545-10550.

(13) Dai, Z.; Wang, Y.; Liu, L.; Liu, X.; Tan, P.; Xu, Z.; Kuang, J.; Liu, Q.; Lou, J.; Zhang, Z. Hierarchical Graphene-Based Films with Dynamic Self-Stiffening for Biomimetic Artificial Muscle. *Adv. Funct. Mater.* **2016**, *26* (38), 7003-7010.